2-15-2001

Secular Variations of OI 5577 Å Airglow in the Mesopause Region Induced by Transient Gravity Wave Packets

Michael P. Hickey Ph.D.
Embry-Riddle Aeronautical University, hicke0b5@erau.edu

R. L. Walterscheid
The Aerospace Corporation

Secular Variations of OI 5577 Å Airglow in the Mesopause Region Induced by Transient Gravity Wave Packets

Michael P. Hickey

Department of Physics and Astronomy, Clemson University, Clemson SC

Richard L. Walterscheid

Space Science Applications Laboratory, The Aerospace Corporation, Los Angeles, CA

Abstract. We employ a 2-dimensional, time-dependent, fully nonlinear model of minor species in the mesopause region and our Spectral Full-Wave Model to simulate the response of minor species and the OI 5577 Å airglow to a gravity wave packet in the mesopause region. Gravity waves affect the time-averaged distribution of minor species in the mesosphere and lower thermosphere (MLT) region through constituent fluxes induced by violation of the non-acceleration conditions due to wave transience and dissipation. In addition, wave perturbed chemistry can induce a flux of chemically active species. Simulations are performed with nominal values of eddy diffusion coefficients in the MLT region, and also using very small values in order to assess the comparative effects of diffusion and wave fluxes. The wave-driven secular variation leads to a strong increase in airglow brightness over a time period of ~2 hrs. In contrast to this, diffusion of minor species leads to a decrease in airglow brightness. The combined effects of the two can lead to secular variations of airglow brightness that resemble those for a long period (> 6 hr) wave. These results have important implications for the interpretation of airglow variations observed in the MLT region.

1.0 Introduction

Accompanying periodic variations in nightglow emission brightness (or temperatures derived therefrom) are variations with no apparent periodicity (i.e., secular) [e.g., *Hecht et al.*, 1995]. These may take the form of large increases or decreases in the apparent mean nightglow emission brightness or temperature. There has been some dispute over whether these secular variations are associated with weak or strong gravity wave activity [*Hecht and Walterscheid*, 1991; *Hostetler and Gardner*, 1994; *Hecht et al.*, 1995]. They may be a result of non-linear effects associated with the interaction of gravity waves with chemically active minor species [*Hecht et al.*, 1995]. This suggestion is based on the results obtained from a steady-state linear model of wave-induced constituent fluctuations [*Walterscheid and Schubert*, 1989]. However, this model did not include the effects of wave dissipation and transience, which provides motivation for the present study.

Recently, *Hickey et al.* [2000b] have shown that gravity wave packets affect the time-averaged distribution of minor species in the mesosphere/lower thermosphere (MLT) region

through constituent fluxes induced by violation of the non-acceleration conditions due to wave transience and dissipation. Mean state forcing is expected whenever the non-acceleration conditions are violated, which are that the waves be linear, conservative, steady, and not encounter a critical level [*Eliassen and Palm*, 1961; *Andrews and McIntyre*, 1976; *Walterscheid*, 1995]. In addition, transport will occur whenever chemistry is able to induce an out of quadrature relation between the vertical velocity and mixing ratio fluctuations [*Walterscheid and Schubert*, 1989]. *Hickey et al.* [2000b] found that downward transport of atomic oxygen (O) was significant, producing ~50% increases in O density below 90 km altitude and depletions in O density of ~20% above 100 km altitude. Additionally, changes in O density due to transient, dissipating gravity waves were considerably greater than changes associated with eddy diffusion acting alone. This paper will demonstrate that in the MLT region, gravity waves can cause a net time-averaged transport of minor species involved in the chemistry of airglow emissions. We apply a rigorous modeling approach to this problem using a 2-D, time-dependent, fully nonlinear model describing the response of minor species in the mesopause region to linear forcing by a gravity wave packet [*Hickey et al.*, 2000b]. We will show that linear gravity waves may play an important role in the distribution of $O(^1S)$ in the MLT region and in the OI Å 5577 brightness due to wave transience and dissipation.

2.0 Model

The numerical model simulates the time variation of minor species number densities subject to the forcing influence of a linear gravity wave packet as described below.

The Spectral Full-Wave Model (SFWM) simulates a time-dependent wave packet using a spectral approach, described in more detail by *Hickey et al.* [2000b]. The basis of this model is a full-wave model [*Hickey et al.*, 1997b, 1998, 2000a] that provides solutions to the Navier-Stokes equations for monochromatic, linear waves propagating in a rotating, non-isothermal atmosphere including the effects of the eddy and molecular diffusion of heat and momentum.

The SFWM used for the calculations presented here requires numerical evaluation of an inverse Fourier transform using 2000 waves (500 positive and 500 negative ω, and 1 positive and 1 negative k, where ω is the wave frequency and k is the horizontal wavenumber). We used a forcing period of 20 minutes, and the periods used to define the frequency spectrum of the packet ranged from ~5 minutes to ~40 hours. The SFWM provides u' and w' (the horizontal and vertical perturbation velocity, respectively), T' (temperature) and ρ'

(density) fluctuations as a function of position and time. The amplitude at the forcing frequency is set to a maximum allowed by the *Orlanski and Bryan* [1969] condition ($u' = \omega_0 / k_0$ in the absence of mean winds, where ω_0 and k_0 are the forcing frequency and horizontal wavenumber, respectively) just above the main airglow region (~ 110 km).

Our 2-D, time-dependent, nonlinear chemistry model solves the coupled continuity equations for the minor species O, $O_2(c'\Sigma_u)$, and $O('S)$ including the effects of advection and diffusion, as described by *Hickey et al.* [2000b]. We use the chemical kinetic parameters given by *Hickey and Walterscheid* [1999]. At the lower boundary (75 km) minor species number densities remain constant, and at the upper boundary (135 km) the species are in diffusive equilibrium. Periodic lateral boundary conditions are used. A time step of 3 seconds, a constant vertical grid spacing of 0.1 km, and a horizontal grid spacing of either 0.5 km or 1 km (corresponding to 60 points in the horizontal direction) provides convergent results.

3.0 Results

We perform experiments using a single wave packet, having a forcing frequency of 20 minutes and a horizontal wavelength (λ_x) of 30 km. The packet parameters are $\tau = 100$ minutes and $\Delta t = 20$ minutes (see *Hickey et al.* [2000b]). We present simulation results for times starting at 2.5 hr for this wave packet because it takes a couple of hours to reach the airglow region. The eddy diffusion profile used in the full-wave model to damp the waves was based on a profile given by *Strobel* [1989]. We describe it as a hyperbolic secant, peaking at 90 km altitude with a maximum nominal value of 100 m² s⁻¹ and with a full-width at half-maximum of 20 km. A similar shape was adopted for the eddy diffusion profile for use in the chemistry part of the model. We used a nominal maximum value for the eddy diffusion of 100 m² s⁻¹, although in order to isolate effects of wave forcing on the secular variations of $O('S)$ the smaller value of 1 m² s⁻¹ was also used.

Figure 1 shows the altitude profile of the amplitude of ρ' for the Fourier component of the wave packet having the

Figure 1a June 21, 2000 5:46:06 PM
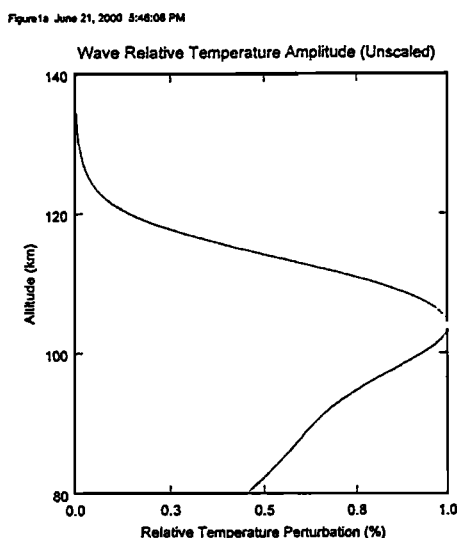
Wave Relative Temperature Amplitude (Unscaled)

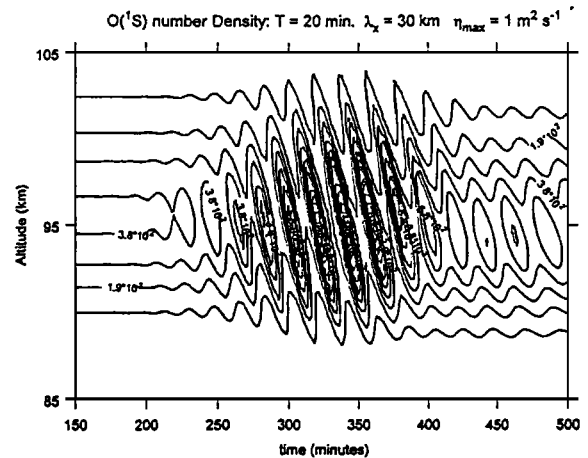Figure 1. Altitude profile of the wave amplitude $|\rho|/\rho$ at the forcing frequency.

Figure 2. $O('S)$ density response to the wave packet as a function of altitude and time.

forcing frequency. The wave is damped mainly by eddy diffusion in the airglow region and by molecular diffusion at higher altitudes. The molecular damping causes the maximum wave amplitude to occur near 105 km altitude. The actual magnitude of the wave is not relevant here, because the entire amplitude profile is rescaled in the model using the *Orlanski and Bryan* [1969] condition, as previously noted. This is equivalent to setting our source amplitude such that the maximum amplitude attained is just that given by the condition $u' = \omega_0 / k_0$. The most significant aspect of these results is that the wave is significantly damped in the vicinity of the $O('S)$ peak near 100 km altitude.

Figure 2 shows the response of the $O('S)$ number density to wave forcing as a function of altitude and time. The downward slope of the phase fronts is consistent with upward energy propagation. At $t \sim 200$ min the wave packet begins to perturb $O('S)$ near 85 km altitude. Significant perturbations in $O('S)$ occur near the $O('S)$ peak (~ 96 km altitude) for times around 250 min. Maximum perturbations in $O('S)$ number density (approaching 100 %) occur in this region at t ~ 350 min.

The OI 5577 brightness as observed at the ground was calculated by integrating the OI 5577 volume emission rate (VER) over altitude, where the VER is equal to the radiation transition probability (1.08 s⁻¹) times the $O('S)$ number density. Figure 3a shows relative density perturbations ($|\rho'|/\bar{\rho}$) at z = 100 km and the *OI 5577* airglow brightness as a function of time at the first horizontal grid position for η_{max} = 1 m² s⁻¹. The OI 5577 brightness has a fluctuating part and a secular variation. We calculate the secular variation by calculating a running average of OI 5577 over time using a window length equal to the forcing period (20 min). The difference between OI 5577 and the secular variation is the fluctuating part. The relative density fluctuation ($|\rho'|/\bar{\rho}$, right hand axis, short-dashed curve) peaks at about 350 minutes with a value of almost 2 %. The initial part of the disturbance (times less than 350 min) is characterized by an amplitude that increases with increasing time, and is associated with the faster wave components of the packet. For times greater than about 430 minutes, the amplitude appears to become constant. This part of the wave packet is comprised of the slower wave components, leading to a slow decay of the packet. At much greater times (not shown) the amplitude does decrease. The
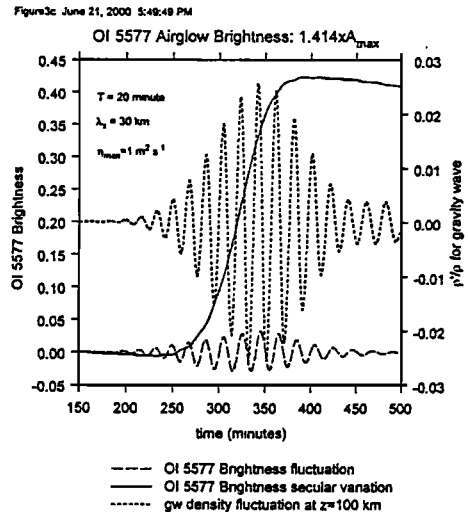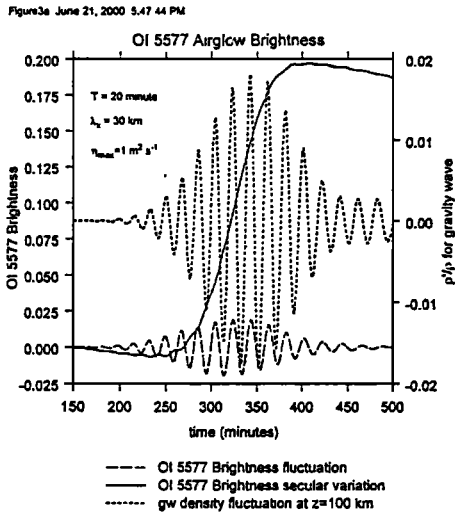
Figure3a June 21, 2000 5.47 44 PM

OI 5577 Airglow Brightness

--- OI 5577 Brightness fluctuation
— OI 5577 Brightness secular variation
······ gw density fluctuation at z=100 km

Figure3c June 21, 2000 5:49:49 PM

OI 5577 Airglow Brightness: 1.414xA$_{max}$

--- OI 5577 Brightness fluctuation
— OI 5577 Brightness secular variation
······ gw density fluctuation at z=100 km

Figure 3a. Relative density perturbations ($|\rho|/\rho$) at z = 100 km and the OI 5577 airglow brightness (secular variation and fluctuation) as a function of time at the first horizontal grid position for $\eta_{max} = 1$ m^2 s^{-1}.

OI 5577 brightness shows a linear secular increase with increasing time (solid line). This increase is associated with the downward transport of O, due to eddy diffusion and associated with wave-driven secular variations, and its subsequent conversion to $O('S)$. Fluctuations in OI 5577 brightness (long-dashed curve) are typically a few percent. At long times the fluctuation amplitude approaches zero because the slower wave components in the packet have short vertical wavelengths, leading to strong line-of-sight cancellation through the airglow layer [e.g., Swenson and Gardner, 1998; Hickey and Walterscheid, 1999].

Figure 3b shows results similar to those of Figure 3a except with increased eddy diffusion in the chemistry model (the maximum value is 100 m^2 s^{-1}). The secular variation of OI 5577 (solid line) initially decreases due to the effects of eddy diffusion. The eddy diffusion causes down-gradient transport of all minor species, which is upward on the layer top side and downward on the layer bottom side. At times near 250 minutes the effects associated with eddy diffusion

Figure3b June 21, 2000 5:48:43 PM

OI 5577 Airglow Brightness

--- OI 5577 Brightness fluctuation
— OI 5577 Brightness secular variation
······ gw density fluctuation at z=100 km

Figure 3b. Similar to Figure 3a except for $\eta_{max} = 100$ m^2 s^{-1}.

Figure 3c. Similar to Figure 3a except for amplitude increased by a factor of $\sqrt{2}$.

become overwhelmed by wave transport effects, and the airglow brightens in a similar fashion to the previous case of low eddy diffusion (Figure 3a). However, the maximum brightening is not as large as before due to the stronger mitigating influence of eddy diffusion. Finally, after wave transport effects wane ($t \sim 400$ minutes), the effects of eddy diffusion again lead to a reduction in airglow brightness. During the approximate 6 hr time interval, secular variations of OI 5577 brightness associated with wave forcing and eddy diffusion resemble those that could be plausibly ascribed to a large amplitude, long period wave. The amplitude of the airglow brightness fluctuations (long dashed curve) is not significantly affected by the effects of eddy diffusion in the chemistry model.

Figure 3c shows similar results to those of Figure 3a except that the amplitude of the wave packet has been increased by a factor of $\sqrt{2}$. The airglow brightness fluctuations also increase by a factor of $\sqrt{2}$, and as expected, the secular variation increases by a factor of approximately 2 because nonlinear flux terms are proportional to the square of the wave amplitude.
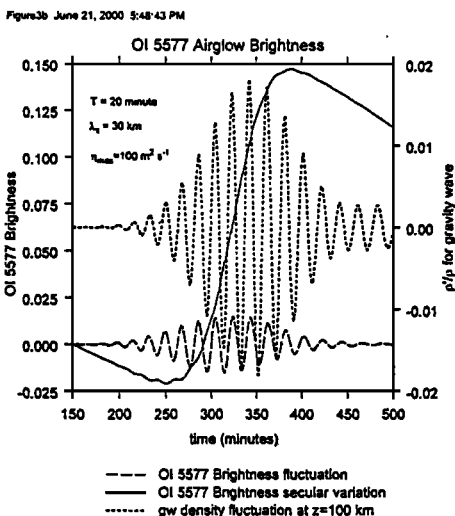
Figure 4 shows $O('S)$ number density plotted as a function of altitude at the final time for several simulations (see Figure caption). The wave packet has a significant effect on the distribution of $O('S)$ (short-dashed curve). At altitudes above about 96 km (the height of the original $O('S)$ peak) $O('S)$ densities are reduced, while at lower altitudes $O('S)$ densities are increased. These effects become larger when the amplitude of the wave is increased by a factor of $\sqrt{2}$ (dashed-three-dotted curve).

4.0 Summary/Conclusions

We have described a model describing the time-dependent, non-linear response of the airglow to dynamical forcing by a gravity wave packet. We find that in addition to causing large fluctuations of the minor species, the wave packet also causes a large secular variation driven by wave transience and dissipation. With the nominal value of $\eta_{max} = 100$ m^2 s^{-1}, the distribution of $O('S)$ in the MLT region appears to be far more influenced by wave transport effects than by the effects of eddy diffusion. The wave-driven secular variation leads to a
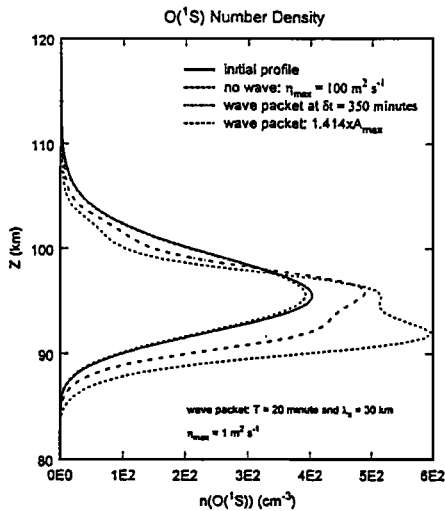
Figure 4. $O(^1S)$ profiles after different simulations. Initial profile (solid curve); effects of chemistry and eddy diffusion only, with $\eta_{max} = 100$ m^2 s^{-1} (thick small dashed curve); wave packet at $t = 500$ minutes (dashed-dotted curve); and wave packet at $t = 500$ minutes and amplitude increased by a factor of $\sqrt{2}$ (long dashed curve).

strong increase in airglow brightness over a time period of about 2 hrs. In contrast to this, the effects of diffusion lead to a decrease in airglow brightness. The combined effects of the two can lead to secular variations of airglow brightness that resemble those for a long period (> 6 hr) wave. These results have important implications for the interpretation of airglow variations observed in the MLT region because it is possible that such variations could be misinterpreted as being due to long period waves. Additionally, we find that the greatest secular variations appear to be associated with the smallest OI 5577 airglow fluctuations (i.e., the waves of smallest λ_z suffer the greatest effects of cancellation in the airglow). The secular variation is made irreversible by wave dissipation and chemistry.

5.0 References

Andrews, D. G., and M. E. McIntyre, Planetary waves in horizontal and vertical shears: the generalized Eliassen and Palm relation and the mean zonal acceleration, *J. Atmos. Sci., 33*, 2031-2048, 1976.

Eliassen, A., and E. Palm, On the transfer of energy in stationary mountain waves, *Geophys. Publ., 22*(3), 1-13, 1961.

Hecht, J. H., and R. L. Walterscheid, Observations of the OH Meinel (6,2) and O$_2$ atmospheric (0,1) nightglow emissions from Maui during the ALOHA-90 campaign, *Geophys. Res. Lett., 18*, 1341, 1991.

Hecht, J. H., S. K. Ramsay-Howat, R. L. Walterscheid, and J. R. Isler, Observations of variations in airglow emissions during ALOHA-93, *Geophys. Res. Lett., 22*, 2817, 1995.

Hickey, M. P., R. L. Walterscheid, M. J. Taylor, W. Ward, G. Schubert, Q. Zhou, F. Garcia, M. C. Kelley, and G. G. Shepherd, A numerical calculation of gravity waves imaged over Arecibo during the 10-day January 1993 campaign, *J. Geophys. Res., 102*, 11,475, 1997b.

Hickey, M. P., and R. L. Walterscheid, A Note on Gravity Wave-Driven Volume Emission Rate Weighted Temperature Perturbations Inferred from O$_2$ Atmospheric and O I 5577 Airglow Observations, *J. Geophys. Res., 104*, 4279, 1999.

Hickey, M. P., M. J. Taylor, C. S. Gardner, and C. R. Gibbons, Full-wave Modeling of Small-Scale Gravity Waves Using Airborne Lidar and Observations of the Hawaiian Airglow (ALOHA-93) O(^{1}S) Images and Coincident Na wind/temperature Lidar Measurements, *J. Geophys. Res., 103*, 6439, 1998.

Hickey, M. P., R. L. Walterscheid, and G. Schubert, Gravity wave heating and cooling in Jupiter's thermosphere, *Icarus, 148*, 266, 2000a.

Hickey, M. P., R. L. Walterscheid, and P. G. Richards, Secular variations of atomic oxygen in the mesopause region induced by transient gravity wave packets, *Geophys. Res. Lett., 27*, 3599, 2000b.

Hostetler, C. A., and C. S. Gardner, Observations of horizontal and vertical wave number spectra of gravity wave motions in the stratosphere and mesosphere over the mid pacific, *J. Geophys. Res., 99*, 1283, 1994.

Orlanski, I., and K. Bryan, Formation of thermocline step structure by large amplitude internal gravity waves, *J. Geophys. Res., 74*, 6975-6983, 1969.

Strobel, D. F., Parameterization of linear wave chemical transport in planetary atmospheres by eddy diffusion, *J. Geophys. Res., 86*, 9806-9810, 1981.

Swenson, G. R., and C. S. Gardner, Analytic models for the responses of the mesospheric OH* and Na layers to atmospheric gravity waves, *J. Geophys. Res., 103*, 6271, 1998.

Walterscheid, R. L., Gravity wave mean state interactions in the upper mesosphere and lower thermosphere, in *The Upper Mesosphere and Lower Thermosphere: A Review of Experiment and Theory*, ed. M. Johnson and T. L. Killeen, Geophysical Monograph 87, American Geophysical Union, 1995.

Walterscheid, R. L., and G. Schubert, Gravity wave fluxes of O$_3$ and OH at the nightside mesopause, *Geophys. Res. Lett., 16*, 719-722, 1989.

M.P. Hickey, Department of Physics and Astronomy, Clemson University, Clemson, SC 29634-0978. (e-mail: hickey@hubcap.clemson.edu)

R.L. Walterscheid, Space Science Application Laboratory, The Aerospace Corporation, Los Angeles, CA 90009.